Int. J. Solids Structures Vol. 18, No. 8, pp. 685–698, 1982
Printed in Great Britain.

0020-7683/82/080685-14$03.00/0
Pergamon Press Ltd.

VARIATIONAL ESTIMATES FOR DISPERSION AND ATTENUATION OF WAVES IN RANDOM COMPOSITES—II

ISOTROPIC COMPOSITES

D. R. S. TALBOT and J. R. WILLIS

School of Mathematics, Bath University, Bath BA2 7AY, England

(*Received* 24 *July* 1981)

Abstract—The general formulae derived in Part I are developed explicitly for an isotropic matrix containing spherical inclusions, and for cubic polycrystals displaying overall isotropy. Results are sensitive to the choice of comparison material; subject to certain limitations the self-consistent choice appears generally to be best. For a matrix containing spheres, the structure factors introduced in Part I are evaluated in terms of similar factors, associated with the radial distribution function. Polycrystals are modelled by a cell structure, so that two-point statistics are also determined by a single radial function. It is suggested that the structure factors associated with these radial functions could be inferred for real materials by experimental study of wave dispersion and attenuation.

1. INTRODUCTION

This paper develops in detail some implications of the general formulae given in the preceding paper[1]. For ease of reference, this is designated I in the sequel, and equations from it are given the prefix I. A fairly wide class of isotropic composites is considered which includes, as special cases, both matrix/inclusion composites and polycrystalline aggregates. The principal simplifying feature displayed by this class is that the two point probabilities P_{rs} are isotropic. This, coupled with the choice of an isotropic comparison material, allows all the integrals given in I to be evaluated explicitly, except for those that define the geometric structure factors Λ'_{rs}, Λ_{rs}, which depend upon the detailed form chosen for the two-point probabilities P_{rs}.

Two examples are considered particularly. The long-wavelength wave speeds, and the corrections for dispersion and attenuation Q', Q, are worked out for a matrix containing spheres and for a polycrystalline aggregate of cubic crystals. Detailed results are given for glass spheres in an epoxy matrix, for which experimental results have been obtained by Kinra *et al.*[2], and for polycrystalline copper, alpha-iron and nickel. The long-wavelength wave speeds, and the perturbations Q, Q', are all sensitive to the choice of comparison material; it is suggested that the self-consistent choice for L_0 is generally likely to be best.

2. GENERAL IMPLICATIONS OF ISOTROPY

The results given in Paper I can be made progressively more explicit, as more simplifying features are introduced. Suppose, first, just that the two-point probabilities, $P_{sr}(x', x)$, in addition to being translation-invariant, also have isotropic form, so that they depend upon $|x - x'|$ only. Then, as shown in [3], the constants A_{rs} given by (I, 4.6) reduce to the form

$$A_{rs} = P(P_r\delta_{rs} - P_rP_s), \tag{2.1}$$

the constant tensor P having components

$$P_{pqij} = \frac{1}{4\pi^2}\sum_{N=1}^{3}\int_{|\xi|=1} \mathrm{d}S\, \frac{\xi_q U_p^N U_i^N \xi_j}{\rho_0 c_N^2}\bigg|_{(ij)(pq)}. \tag{2.2}$$

This simplification occurs because, when P_{sr} is isotropic, the static kernel Γ^∞ behaves like P times a delta-function, with P representing the integral of Γ^∞ over a sphere of any radius, centred on the origin. When A_{rs} take the form (2.1), equations (I, 4.2) have the explicit solution

$$\tau_r = S_r\langle e\rangle, \tag{2.3}$$

where

$$S_r = (L_r - L_0)[I + P(L_r - L_0)]^{-1}\left\{\sum P_s[I + P(L_s - L_0)]^{-1}\right\}^{-1}. \tag{2.4}$$

Correspondingly, the Hashin–Shtrikman estimate (I, 4.8) for the tensor of overall moduli becomes

$$\tilde{L} = \sum P_r L_r[I + P(L_r - L_0)]^{-1}\left\{\sum P_s[I + P(L_s - L_0)]^{-1}\right\}^{-1}. \tag{2.5}$$

The result was first given at this level of generality by Walpole [4].

The other simplifying features that follow from the assumption of isotropy of P_{sr} are that the integrand in the definition (I, 4.17) of Λ_{sr} depends upon the radial variable alone and, correspondingly, (I, 4.16) shows that $\Lambda'_{sr}(\xi)$ is independent of the direction of ξ. Thus, if ξ is not a unit vector,

$$\Lambda'_{sr}(\xi) = |\xi|^{-1}\Lambda'_{sr} \tag{2.6}$$

where, on the right side of (2.6), Λ'_{sr} represents the value of Λ'_{sr} when $|\xi| = 1$, and so is independent of ξ. The derivatives that appear in (I, 4.19) and (I, 4.20) are now easy to evaluate explicitly:

$$(n.\nabla_\xi)\Lambda'_{sr}(\xi) = -\frac{(n.\xi)}{|\xi|^3}\Lambda'_{sr} \tag{2.7}$$

$$(n.\nabla_\xi)^2\Lambda'_{sr}(\xi) = \left\{\frac{3(n.\xi)^2}{|\xi|^5} - \frac{1}{|\xi|^3}\right\}\Lambda'_{sr} \tag{2.8}$$

The assumption of isotropy of P_{sr} does not by itself imply overall isotropy of the composite, since all of the L_r may still be anisotropic and display preferred orientations. If, however, the L_r are chosen so that the composite is elastically isotropic, it is sensible to choose the moduli L_0 of the comparison material to have isotropic form. In this case, L_0 is specified by a bulk modulus κ_0 and a shear modulus μ_0 and it is convenient to employ a symbolic notation introduced by Hill [5]:

$$L_0 = (3\kappa_0, 2\mu_0). \tag{2.9}$$

The tensor P is correspondingly isotropic; completing the algebra gives

$$P = \left(\frac{1}{3\kappa_0 + 4\mu_0}, \frac{3(\kappa_0 + 2\mu_0)}{5\mu_0(3\kappa_0 + 4\mu_0)}\right). \tag{2.10}$$

Then, if all of the phases of the composite are isotropic, so $L_r = (3\kappa_r, 2\mu_r)$, eqn (2.5) gives

$$\tilde{L} = (3\tilde{\kappa}, 2\tilde{\mu}), \tag{2.11}$$

where

$$\tilde{\kappa} = \sum P_r\kappa_r\left(\frac{3\kappa_0 + 4\mu_0}{3\kappa_r + 4\mu_0}\right)\left\{\sum P_s\left(\frac{3\kappa_0 + 4\mu_0}{3\kappa_s + 4\mu_0}\right)\right\}^{-1},$$

$$\tilde{\mu} = \sum P_r\mu_r\left(\frac{5\mu_0(3\kappa_0 + 4\mu_0)}{6\mu_r(\kappa_0 + 2\mu_0) + \mu_0(9\kappa_0 + 8\mu_0)}\right)\left\{\sum P_s\frac{5\mu_0(3\kappa_0 + 4\mu_0)}{6\mu_s(\kappa_0 + 2\mu_0) + \mu_0(9\kappa_0 + 8\mu_0)}\right\}^{-1}. \tag{2.12}$$

Expressions for $\tilde{\kappa}$, $\tilde{\mu}$ appropriate to a polycrystal are given later.

The low-frequency dispersion relation (I, 4.12) now shows that the composite will support longitudinal waves, with wave speed

$$\omega/k_1 = \tilde{\alpha} = ([\tilde{\kappa} + 4\tilde{\mu}/3])/\tilde{\rho})^{1/2} \tag{2.13}$$

and shear waves, with wave speed

$$\omega/k_2 = \omega/k_3 = \tilde{\beta} = (\tilde{\mu}/\tilde{\rho})^{1/2}. \tag{2.14}$$

The associated displacements $\langle u \rangle_N$ have the form

$$\langle u \rangle_N = Am_N \exp(-i[k_N(n.x) + \omega t]), \tag{2.15}$$

where m_N, $N = 1, 2, 3$ are orthonormal, with

$$m_1 = n \quad \text{and} \quad m_2.n = m_3.n = 0 \tag{2.16}$$

and A is an arbitrary amplitude.

The perturbations Q, Q' to the low-frequency dispersion relation involve the polarizations τ_r, π_r and the constants $A_{rs}^{(kk)} \ldots E_{rs}$, defined by eqns (I, 4.25–4.31). The constant tensors D_{rs}, E_{rs} were worked out, in a slightly different context, by Willis[6]. They are isotropic, as are also $A_{rs}^{(\omega\omega)}$ and C_{rs}; the remaining tensors are expressible in terms of isotropic tensors, contracted with n. The results are listed.

$$A_{rs}^{(kk)} = A^{(kk)}\Lambda'_{sr},\ A_{rs}^{(\omega\omega)} = A^{(\omega\omega)}\Lambda'_{sr},\ B_{rs} = B\Lambda'_{sr},$$

$$C_{rs} = C\Lambda'_{sr},\ D_{rs} = D\Lambda_{sr},\ E_{rs} = E\Lambda_{sr}, \tag{2.17}$$

where

$$A^{(\omega\omega)} = \left(\frac{1}{6\pi\rho_0\alpha_0{}^4}, \frac{1}{10\pi\rho_0\alpha_0{}^4}\left(\frac{1}{\sigma_0{}^4} + \frac{2}{3}\right)\right), \tag{2.18}$$

$$D = \left(\frac{1}{12\pi\rho_0\alpha_0{}^3}, \frac{1}{20\pi\rho_0\alpha_0{}^3}\left(\frac{1}{\sigma_0{}^3} + \frac{2}{3}\right)\right), \tag{2.19}$$

$$(C)_{pi} = \frac{1}{6\pi\rho_0\alpha_0{}^2}\left(\frac{2}{\sigma_0{}^2} + 1\right)\delta_{pi}, \tag{2.20}$$

$$(E)_{pi} = \frac{1}{12\pi\rho_0\alpha_0{}^3}\left(\frac{2}{\sigma_0{}^3} + 1\right)\delta_{pi}. \tag{2.21}$$

In (2.18) to (2.21), $\alpha_0 = [(\kappa_0 + 4\mu_0/3)/\rho_0]^{1/2}$ is the speed with which longitudinal waves would travel in the comparison material and $\sigma_0 = \beta_0/\alpha_0$, where $\beta_0 = (\mu_0/\rho_0)^{1/2}$ is the corresponding shear wave speed. The remaining constants are expressible in the forms

$$(B)_{pqi} = B^*_{pqij}n_j, \tag{2.22}$$

where

$$B^* = \left(\frac{1}{6\pi\rho_0\alpha_0{}^2}, \frac{1}{10\pi\rho_0\alpha_0{}^2}\left(\frac{1}{\sigma_0{}^2} + \frac{2}{3}\right)\right), \tag{2.23}$$

and

$$A^{(kk)} = A^* - \frac{1}{35\pi\rho_0\alpha_0{}^2}\left(\frac{10}{3} - \frac{1}{\sigma_0{}^2}, \frac{4}{3} + \frac{1}{\sigma_0{}^2}\right), \tag{2.24}$$

where

$$A^*_{pqij} = \frac{1}{35\pi\rho_0\alpha_0^2}\left\{\left(1-\frac{1}{\sigma_0^2}\right)\left(\delta_{pq}n_in_j+\delta_{ij}n_pn_q\right)+\left(4+\frac{3}{\sigma_0^2}\right)n_q\delta_{pi}n_j\Big|_{(pq\times ij)}\right\}. \tag{2.25}$$

This completes the assembly of the constants relevant to all isotropic composites. Particular cases are disucssed in the sections that follow.

3. A MATRIX CONTAINING SPHERICAL INCLUSIONS

Consider first an isotropic matrix containing a distribution of spherical inclusions. The inclusion phase is labelled 1, so that the inclusions have moduli $L_1 = (3\kappa_1, 2\mu_1)$, while the matrix has moduli $L_2 = (3\kappa_2, 2\mu_2)$. The overall moduli $\tilde{L}$ have already been given by (2.11), (2.12) and so attention is focussed upon the calculation of Q, Q'. The probabilities P_r, P_{rs} satisfy the relations

$$P_1 + P_2 = 1,\ P_{11} + P_{12} = P_1,\ P_{12} + P_{22} = P_2 \tag{3.1}$$

and these allow the "structure factors" Λ_{rs}, Λ'_{rs} to be expressed in terms of Λ_{11}, Λ'_{11}. It follows, in fact, that eqns (I, 4.41) and (I, 4.42) reduce to

$$\begin{aligned} Q' = -\frac{\Lambda'_{11}}{m\tilde{L}(n)m}&[(\tau_1-\tau_2)(A^{(kk)}+\gamma^2A^{(\omega\omega)})(\tau_1-\tau_2)\\ &+2\gamma(\tau_1-\tau_2)B(\pi_1-\pi_2)+\gamma^2(\pi_1-\pi_2)C(\pi_1-\pi_2)], \end{aligned} \tag{3.2}$$

$$Q = -\frac{\Lambda_{11}\gamma^2\omega}{m\tilde{L}(n)m}[(\tau_1-\tau_2)D(\tau_1-\tau_2)+(\pi_1-\pi_2)E(\pi_1-\pi_2)], \tag{3.3}$$

where

$$\gamma = \omega/k \tag{3.4}$$

and k, m take the values k_N, m_N appropriate to the branch of the dispersion relation under consideration. From (2.3), now,

$$(\tau_1-\tau_2) = (S_1-S_2)\langle e\rangle, \tag{3.5}$$

where

$$\langle e\rangle_{ij} = -ik(m_in_j+m_jn_i)/2, \tag{3.6}$$

and it can be shown, either from (2.4) or directly from eqns (I, 4.6), that

$$S_1 - S_2 = [I+(P_2L_1+P_1L_2-L_0)P]^{-1}(L_1-L_2) \tag{3.7}$$

or, explicitly,

$$S_1-S_2 = \left(\frac{3(\kappa_1-\kappa_2)(3\kappa_0+4\mu_0)}{3(P_2\kappa_1+P_1\kappa_2)+4\mu_0}, \frac{10(\mu_1-\mu_2)\mu_0(3\kappa_0+4\mu_0)}{6(P_2\mu_1+P_1\mu_2)(\kappa_0+2\mu_0)+\mu_0(9\kappa_0+8\mu_0)}\right). \tag{3.8}$$

From (I, 4.3),

$$\pi_1-\pi_2 = -i\omega(\rho_1-\rho_2)m. \tag{3.9}$$

This completes the specification of the tensors that appear in (3.2), (3.3). They are easy to manipulate, on account of their isotropic structure and, furthermore, the wave normal n may be

taken to have components (1, 0, 0), without loss of generality. Correspondingly, m_1, m_2 have components (1, 0, 0), (0, 1, 0) respectively and there is no need to consider m_3.

There remains the task of evaluating the structure factors Λ_{11}, Λ'_{11}. This is complicated slightly by the fact that a distribution of inclusions is most naturally described in terms of a number density n_1 and a pair distribution function $g(x)$ (which, for the case being considered, depends upon $|x|$ only and is usually called the radial distribution function). If the inclusions all have radius a, the number density n_1 is related to P_1 by

$$P_1 = 4\pi a^3 n_1/3 \tag{3.10}$$

and the pair distribution function is related to the probability density $P(x|x')$ for finding an inclusion centred at x, given that a different inclusion is centred at x', by

$$P(x|x') = n_1 g(x - x'). \tag{3.11}$$

In the present case, therefore, $g(x) = 0$ when $|x| < 2a$, since inclusions cannot overlap, and $g(x) \to 1$ as $|x| \to \infty$, since no long-range order is assumed.

In preparation for evaluating Λ_{11}, Λ'_{11}, it is noted that $P_{11}(x, 0)$, the probability that both x and 0 lie in an inclusion, is given as

$$P_{11}(x, 0) = n_1 v(x) + n_1^2 \int_{B(0,a)} dx' \int_{B(x,a)} dx'' g(x'' - x'), \tag{3.12}$$

where $B(x, a)$ denotes the sphere of radius a, centred at x and $v(x)$ denotes the volume of the intersection of $B(0, a)$ and $B(x, a)$. The first term on the right side of (3.12) is the probability that x, 0 lie in the same inclusion and the second is the probability that they lie in different inclusions. The structure factor Λ_{11} now follows as

$$\Lambda_{11} = n_1 \int v(x)\, dx + n_1^2 \int dx \int_{B(0,a)} dx' \int_{B(x,a)} dx''[g(x'' - x') - 1]. \tag{3.13}$$

The first integral on the right side of (3.13) is elementary and the second can be reduced by the change of variable $x'' = x' + u$, to give the result

$$\Lambda_{11} = \left(\frac{4\pi a^3}{3}\right) P_1 \Lambda, \tag{3.14}$$

where

$$\Lambda = 1 + n_1 \int du[g(u) - 1]; \tag{3.15}$$

the factor Λ appeared in [6]. Evaluation of Λ'_{11} is less straightforward; the result

$$\Lambda'_{11} = \frac{4\pi a^2}{5} P_1 \Lambda', \tag{3.16}$$

where

$$\Lambda' = 1 + \frac{13}{112} P_1 + \frac{13\pi a}{6} n_1 \int_0^\infty r\, dr[g(x) - 1], \tag{3.17}$$

relies upon the fact that $g(x)$ depends upon $r = |x|$ only. The factor Λ' is plotted against concentration P_1 in Fig. 1 for the "well-stirred" distribution defined by

$$\begin{aligned} g(x) &= 0, \quad |x| < 2a \\ &= 1, \quad |x| > 2a \end{aligned} \tag{3.18}$$

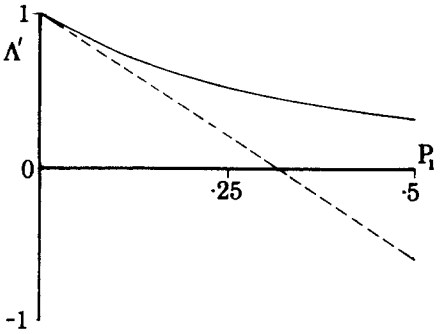

Fig. 1. Plot of the structure factor Λ' against concentration P_1, for the "well-stirred" approximation (----) and for the Percus-Yevick approximation for the radial distribution function (————).

and for the Perkus–Yevick hard sphere approximation of statistical mechanics[7]: for the latter model, the Laplace transform of $rg(r)$ is known explicitly[8] and Λ' follows from its small-argument expansion. Corresponding plots of Λ were given in [6].

The exact predictions of the formulae that have been presented depend upon the choice of comparison material. In [6], the comparison material was identified with the matrix and the quasicrystalline approximation of Lax[9] was applied to close the hierarchy associated with the operator eqns (I, 2.8, 2.9). With this choice of comparison material, the present formulation gives estimates for $\tilde{L}$ and Q that agree precisely with the corresponding results in [6] (in which the symbol Q had a slightly different meaning). The real perturbation Q' was not calculated in [6], however. The most significant advantage of the present scheme, in addition to its variational foundation, is that it allows other choices of comparison material. In particular, L_0 may be chosen so that $L_r - L_0$ is positive semi-definite and $\rho_r - \rho_0 \geqslant 0$ for each r, when the associated $\tilde{L}$ is the Hashin–Shtrikman lower bound, or so that $L_r - L_0$ is negative semi-definite and $\rho_r - \rho_0 \leqslant 0$ for each r, when $\tilde{L}$ is the Hashin–Shtrikman upper bound[10]. Alternatively, L_0 may be chosen self-consistently, so that

$$\tilde{L}(L_0) = L_0. \tag{3.19}$$

It was shown in [3] that this prescription (which can also be applied for any two-point probabilities P_{rs}) reproduces the self-consistent estimates formulated by Hershey[11], Hill[12] and Budiansky[13]. It is natural to associate with (3.19) the choice

$$\rho_0 = \tilde{\rho} = P_1\rho_1 + P_2\rho_2. \tag{3.20}$$

Results corresponding to these three choices of comparison material are displayed in Figs. 2–4 for a composite comprising an epoxy matrix with embedded glass spheres, which has been studied experimentally by Kinra, Petraitis and Datta[2]. For this material, the "lower bound" and "upper bound" estimates for $\tilde{L}$ are produced by identifying the comparison material with the matrix and the inclusions, respectively.

Figure 2 shows (in unbroken lines) plots of long-wavelength estimates $\tilde{\alpha}$ for the speed of longitudinal waves, against volume concentration of inclusions. The material properties

$$\kappa_1 = 43.09,\ \mu_1 = 25.98\ \text{GPa},\ \rho_1 = 2.47\ \text{g cm}^{-3}$$

$$\kappa_2 = 5.205,\ \mu_2 = 1.482\ \text{GPa},\ \rho_2 = 1.18\ \text{g cm}^{-3}$$

were adopted, to conform with [2]. The upper bound curve ($L_0 = L_1$) and the lower bound curve ($L_0 = L_2$) are rather far apart, as would be expected for a composite with such large differences in moduli. The self-consistent estimate, obtained by choosing $L_0 = \tilde{L}$, lies between the bounds and probably provides the best of the three estimates for $\tilde{\alpha}$ up to moderate concentrations, though the observation[13] that the self-consistent estimate for the shear modulus of an imcompressible matrix containing rigid spheres becomes unbounded at a volume concentration 0.4 might suggest, for the present composite, that the self-consistent $\tilde{\alpha}$ is an overestimate at

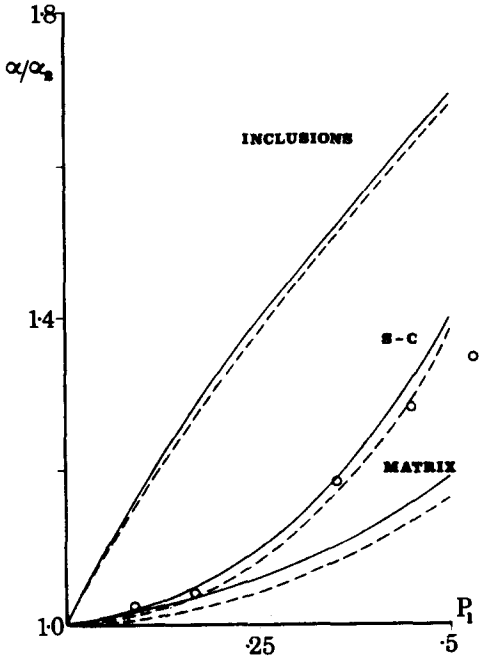

Fig. 2. Long-wavelength estimates $\tilde{\alpha}$ (unbroken lines) of the longitudinal wave speed in an epoxy matrix containing glass spheres, plotted against volume concentration spheres, for different choices of comparison material. The broken lines show estimates allowing for the perturbation Q', when the spheres have radius 150 μm and conform to Percus–Yevick statistics, and the frequency of the wave is 0.8 MHz. Experimental points taken from [2] are also shown. Results are normalized to the wave speed α_2 of the matrix.

such concentrations. Also displayed on Fig. 2 are corrections due to dispersion: the broken lines represent estimates α' of phase velocities, allowing for the first-order correction Q' through the formula

$$\alpha' \sim \tilde{\alpha}(1 - Q'/2). \tag{3.21}$$

The correction term Q' is proportional to ω^2 and also depends upon the radial distribution function $g(x)$ through the factor Λ'. The corrections shown assume a frequency of 0.8 MHz and a Perkus–Yevick distribution of spheres, all of radius $a = 150\,\mu$m. The results demonstrate a tendency for phase velocity to decrease with frequency. Experimental points, taken from a figure in [2], are also shown; the composite that was tested in [2] had the properties assumed in the calculation except, of course, that its radial distribution function was unknown. Comparison

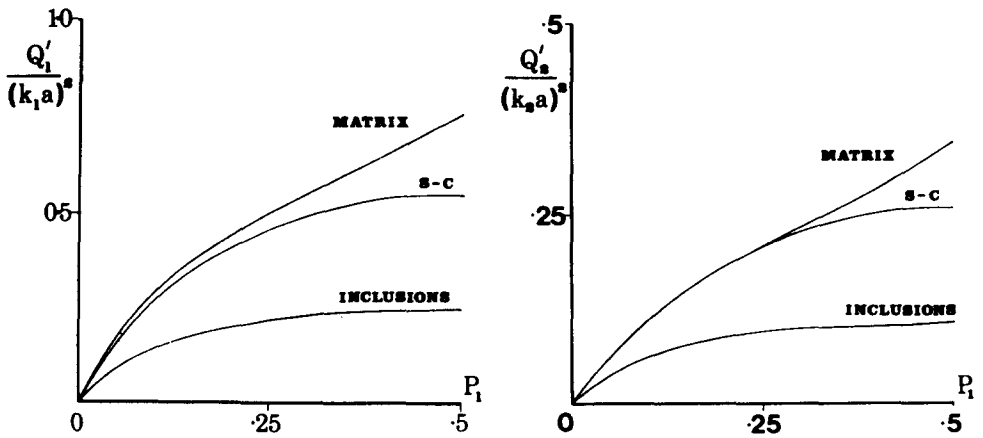

Fig. 3. (a) Estimates of the correction factor Q_1', plotted against concentration of spheres, for the composite described in Fig. 2. (b) Estimates of the correction factor Q_2', plotted against concentration spheres, for the same composite.

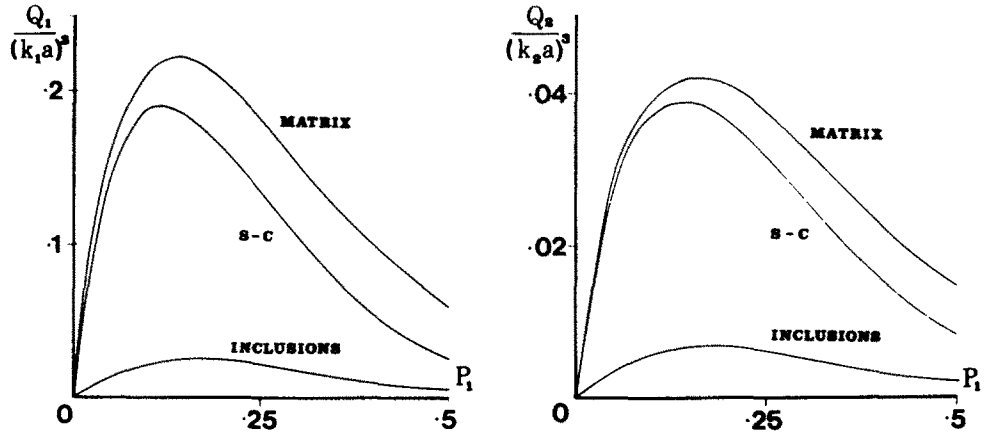

Fig. 4. (a) Estimates of the correction factor Q_1, plotted against concentration of spheres. (b) Estimates of the correction factor Q_2, plotted against concentration of spheres.

between theory and experiment tends to support the self-consistent choice of L_0. Corresponding results have been obtained for shear waves but these are not displayed.

It has been suggested[14, 15] that the radii of inclusions might be estimated from measurements of dispersion and attenuation. The formulae given in this work demonstrate that, in fact, such measurements are sensitive to $g(x)$ as well as to inclusion size and concentration. Normalized plots of the corrections Q_1' for longitudinal waves and Q_2' for shear waves are shown against concentration, for the three choices of comparison material, in Figs. 3(a, b) respectively. The assumed material properties are the same as for Fig. 2, including the Percus–Yevick $g(x)$. Corresponding plots of Q_1, Q_2 are shown in Figs. 4(a, b). The estimates vary with choice of comparison material but we would speculate that those obtained with the self-consistent choice are the most realistic.

4. POLYCRYSTALS

This section considers a particular "cell" model for a polycrystalline aggregate. In general, a "cell" model is defined by subdividing the space occupied by the material into cells, in such a way that the probability that points x, x' lie in the same cell is $p(x, x')$. Each cell is then assigned a label r, with probability P_r, independently of the labels assigned to other cells. It follows then that

$$P_{rs}(x, x') = P_r\delta_{rs}p(x, x') + P_rP_s(1 - p(x, x')). \tag{4.1}$$

For the case under consideration, the distribution of cells is taken to be statistically uniform and isotropic, so that $p(x, x')$ in fact depends upon $|x - x'|$ only. Also, each cell is to be regarded as a crystal grain, composed of material whose elastic moduli, measured relative to a chosen set of crystallographic axes, are L_c. The label r now defines the orientation of the crystallographic axes and is more appropriately replaced by g, a member of the rotation group $\mathcal{G}$. The moduli L_g of "phase g" are thus obtained by applying the rotation g to L_c. The rotation g may be parametrized by Eulerian angles (θ, ϕ, ψ). Isotropic polycrystals are considered, for which all rotations g occur with equal probability, so that (4.1) is replaced by the density

$$P_{gg'}(x, x') = \frac{1}{8\pi^2}\delta(g - g')p(|x - x'|) + \frac{1}{(8\pi^2)^2}(1 - p(|x - x'|)). \tag{4.2}$$

In terms of the Eulerian angles (θ, ϕ, ψ) the element dg takes the form

$$dg = \sin\theta\, d\theta\, d\phi\, d\psi, \tag{4.3}$$

so that $\int_{\mathcal{G}} dg = 8\pi^2$. All previous expressions involving sums become replaced by corresponding integrals over $\mathcal{G}$.

The tensor of overall moduli $\tilde{L}$ follows as such a limit of (2.5), in which the tensors L_0, P are isotropic. Consider the term

$$\hat{L} = \frac{1}{8\pi^2}\int_{\mathcal{G}} dg L_g[I + P(L_g - L_0)]^{-1}. \tag{4.4}$$

This is isotropic and so is characterized by bulk and shear moduli $\hat{\kappa}$, $\hat{\mu}$ which, furthermore, are determined by the invariants

$$\hat{L}_{iikk} = 9\hat{\kappa},\ \hat{L}_{ijij} = 3\hat{\kappa} + 10\hat{\mu}. \tag{4.5}$$

The corresponding invariants of the integrand in (4.4) are, of course, independent of g and so may be evaluated by replacing L_g by L_c, whereupon the integration over $\mathcal{G}$ becomes trivial. The "continuous r" analogue of the inverse operator that appears on the right side of (2.5) may be treated similarly, and $\tilde{L}$ follows without performing any explicit integration over $\mathcal{G}$. All "phases" g of the polycrystal have the same density, ρ say, so that $\tilde{\rho} = \rho$ and, with ρ_0 set equal to ρ, there are no momentum polarizations.

As a first step towards evaluating the perturbations Q, Q', it is noted that the structure factors Λ_{rs}, Λ'_{rs} become replaced by corresponding densities

$$\Lambda_{gg'} = \Lambda\left[\frac{1}{8\pi^2}\delta(g - g') - \frac{1}{(8\pi^2)^2}\right], \tag{4.6}$$

$$\Lambda'_{gg} = \Lambda'\left[\frac{1}{8\pi^2}\delta(g - g') - \frac{1}{(8\pi^2)^2}\right], \tag{4.7}$$

where

$$\Lambda = 4\pi\int_0^\infty p(r)r^2\,dr, \tag{4.8}$$

$$\Lambda' = 2\pi\int_0^\infty p(r)r\,dr. \tag{4.9}$$

The factors Λ, Λ' represent, respectively, the expected volume of a cell and the expected area of its intersection with a plane passing through a specified point, both conditional upon the cell containing that point.

Then, since $\pi_g = 0$, eqn (I, 4.41) gives, with (2.17),

$$Q' = -\frac{\Lambda'}{m\tilde{L}(n)m}\left\{\frac{1}{8\pi^2}\int_{\mathcal{G}} dg\tau_g(A^{(kk)} + \gamma^2 A^{(\omega\omega)})\tau_g - \bar{\tau}(A^{(kk)} + \gamma^2 A^{(\omega\omega)})\bar{\tau}\right\}, \tag{4.10}$$

where τ_g is related to $\langle e\rangle$ by (I, 4.7), with r replaced by g, and

$$\bar{\tau} = \frac{1}{8\pi^2}\int_{\mathcal{G}} dg\tau_g. \tag{4.11}$$

Similarly, from (I, 4.42) and (2.17),

$$Q = -\frac{\Lambda\gamma\omega}{m\tilde{L}(n)m}\left\{\frac{1}{8\pi^2}\int_{\mathcal{G}} dg\tau_g D\tau_g - \bar{\tau}D\bar{\tau}\right\}. \tag{4.12}$$

Equation (4.12) will be considered first, because it is simpler than (4.10). The integral over $\mathcal{G}$ may be expanded to the form

$$\frac{1}{8\pi^2}\int_{\mathcal{G}} dg\tau_g D\tau_g = -\frac{k^2}{8\pi^2}\int_{\mathcal{G}} dg m_i n_j (S_g D S_g)_{ijkl} m_k n_l. \tag{4.13}$$

The integrand is insensitive to rotations and it simplifies upon application of the rotation g^{-1}. Then, the tensor $S_g D S_g$ becomes $S_c D S_c$, D being isotropic, while the vectors m, n become replaced by the rotated vectors $g^{-1}m$, $g^{-1}n$. Therefore, since the integration is over the whole of $\mathcal{G}$ in any case,

$$\frac{1}{8\pi^2}\int_{\mathcal{G}} \mathrm{d}g\tau_g D\tau_g = -\frac{k^2}{8\pi^2}\int_{\mathcal{G}} \mathrm{d}g(gm)_i(gn)_j(S_c D S_c)_{ijkl}(gm)_k(gn)_l. \tag{4.14}$$

That is, the average may be taken instead over all wave orientations, relative to fixed crystallographic axes.

The integral over $\mathcal{G}$ in (4.10) may be transformed similarly, but with the complication that the tensor $A^{(kk)}$ itself depends upon n. Thus, the integrand that results involves products of up to six components of g.

Results will be presented for cases in which L_c has cubic symmetry, so that the relation $\sigma = L_c e$ may be given in the form

$$\sigma_{kk} = 3\kappa_c e_{kk},\ \sigma_{11} - \sigma_{22} = 2\mu_c(e_{11} - e_{22}),\ \sigma_{12} = 2\mu_c' e_{12}, \tag{4.15}$$

with equations for other components of σ obtained by cyclic permutation of the suffixes. With the notation

$$L_c = (3\kappa_c, 2\mu_c, 2\mu_c') \tag{4.16}$$

introduced by Walpole[16], products and inverses can be worked out directly, after which, application of the prescription (4.5) to the terms from which $\tilde{L}$ is composed gives

$$\tilde{\kappa} = \kappa_c, \tag{4.17}$$

$$\tilde{\mu} = \frac{30\mu_c\mu_c'(\kappa_0 + 2\mu_0) + (2\mu_c + 3\mu_c')\mu_0(9\kappa_0 + 8\mu_0)}{(18\mu_c + 12\mu_c')(\kappa_0 + 2\mu_0) + 5\mu_0(9\kappa_0 + 8\mu_0)}. \tag{4.18}$$

The natural choice for κ_0 in (4.18), is $\kappa_0 = \kappa_c$. The choices $\mu_0 = \mu_c$ or μ_c' yield the Hashin–Shtrikman bounds[17] while the self-consistent equation for $\tilde{\mu}$, obtained by setting $\mu_0 = \tilde{\mu}$, is cubic, differing from the original quartic of Hershey[11] by a factor $(8\tilde{\mu} + 9\kappa_c)$.

Now consider the evaluation of Q, from (4.12). First, from (4.11) and (I, 4.7),

$$\bar{\tau} = \bar{S}\langle e\rangle, \tag{4.19}$$

where

$$\bar{S} = \frac{1}{8\pi^2}\int_{\mathcal{G}} \mathrm{d}g S_g = \tilde{L} - L_0, \tag{4.20}$$

from (I, 4.8). This is isotropic and the term $\bar{\tau}D\bar{\tau}$ in (4.12) follows immediately. The integral over $\mathcal{G}$ in (4.12) is best evaluated from (4.14). Using "cubic" notation, it follows from (2.4) that

$$S_c = (0, 2\mu_s, 2\mu_s'), \tag{4.21}$$

where

$$\mu_s = \frac{(\mu_c - \mu_0)[30\mu_c'(\kappa_c + 2\mu_0) + 5\mu_0(9\kappa_c + 8\mu_0)]}{(18\mu_c + 12\mu_c')(\kappa_c + 2\mu_0) + 5\mu_0(9\kappa_c + 8\mu_0)}, \tag{4.22}$$

$$\mu_s' = \frac{(\mu_c' - \mu_0)[30\mu_c(\kappa_c + 2\mu_0) + 5\mu_0(9\kappa_c + 8\mu_0)]}{(18\mu_c + 12\mu_c')(\kappa_c + 2\mu_0) + 5\mu_0(9\kappa_c + 8\mu_0)}. \tag{4.23}$$

Therefore,

$$S_c D S_c = (0, 8\mu_s^2\mu_D, 8(\mu_s')^2\mu_D) \tag{4.24}$$

where, from (2.19),

$$2\mu_D = \frac{1}{20\pi\rho_0\alpha_0^5}\left(\frac{1}{\sigma_0^3}+\frac{2}{3}\right). \tag{4.25}$$

For longitudinal waves, now, $k = k_1$, $m = m_1 = n$ so that $\langle e\rangle_{ij} = -ik_1 n_i n_j$, and $\gamma = \tilde{\alpha}$. Correspondingly,

$$\langle e\rangle(S_c D S_c)\langle e\rangle = -k_1^2\frac{16}{3}\mu_D\{\mu_s^2(n_1^4+n_2^4+n_3^4)+(3(\mu_s')^2-\mu_s^2)(n_1^2n_2^2+n_2^2n_3^2+n_3^2n_1^2)\} \tag{4.26}$$

which gives, upon averaging over all directions n,

$$\frac{1}{8\pi^2}\int_{\mathcal{G}} dg\langle e\rangle(S_g D S_g)\langle e\rangle = -k_1^2\frac{16}{3}\mu_D\left\{\frac{2}{5}\mu_s^2+\frac{3}{5}(\mu_s')^2\right\}. \tag{4.27}$$

Hence, Q_1, the attenuation factor for longitudinal waves, is

$$Q_1 = \frac{2\Lambda\tilde{\alpha}k_1^3}{15\pi\rho^2\alpha_0^5}\left(\frac{1}{\sigma_0^3}+\frac{2}{3}\right)\left\{\frac{2}{5}\mu_s^2+\frac{3}{5}(\mu_s')^2-(\tilde{\mu}-\mu_0)^2\right\}, \tag{4.28}$$

the circular frequency ω having been eliminated by using $\omega = \tilde{\alpha}k_1$. The corresponding result for shear waves may be worked out similarly; it is

$$Q_2 = \frac{\Lambda\tilde{\beta}k_2^3}{10\pi\rho^2\alpha_0^5}\left(\frac{1}{\sigma_0^3}+\frac{2}{3}\right)\left\{\frac{2}{5}\mu_s^2+\frac{3}{5}(\mu_s')^2-(\tilde{\mu}-\mu_0)^2\right\}. \tag{4.29}$$

Evaluation of the factors Q_N' falls into two parts: one, associated with the isotropic part of $A^{(kk)}+\gamma^2A^{(\omega\omega)}$, follows precisely the pattern established above while the other, associated with the term A^* in (2.25), involves the average of $(\tau_{ij}n_j)(\tau_{iq}n_q)$. The results are

$$Q_1' = \frac{\Lambda' k_1^2}{35\pi\rho^2\alpha_0^2\tilde{\alpha}^2}\left\{\frac{4}{3}\left[\frac{7\tilde{\alpha}^2}{\alpha_0^2}\left(\frac{1}{\sigma_0^4}+\frac{2}{3}\right)-2\left(\frac{1}{\sigma_0^2}+\frac{4}{3}\right)\right]\left[\frac{2}{5}\mu_s^2+\frac{3}{5}(\mu_s')^2-(\tilde{\mu}-\mu_0)^2\right]\right.$$
$$\left.+\left(4+\frac{3}{\sigma_0^2}\right)\left[\frac{12}{7}(\mu_s-\mu_s')^2+\frac{24}{5}(\mu_s-\mu_s')(\mu_s'-\mu_s/3)+4(\mu_s'-\mu_s/3)^2-\frac{16}{9}(\tilde{\mu}-\mu_0)^2\right]\right\} \tag{4.30}$$

for longitudinal waves and

$$Q_2' = \frac{\Lambda' k_2^2}{35\pi\rho^2\alpha_0^2\tilde{\beta}^2}\left\{\left[\frac{7\tilde{\beta}^2}{\alpha_0^2}\left(\frac{1}{\sigma_0^4}+\frac{2}{3}\right)-2\left(\frac{1}{\sigma_0^2}+\frac{4}{3}\right)\right]\left[\frac{2}{5}\mu_s^2+\frac{3}{5}(\mu_s')^2-(\tilde{\mu}-\mu_0)^2\right]\right.$$
$$\left.+\left(4+\frac{3}{\sigma_0^2}\right)\left[(\mu_s')^2+\frac{4}{5}\mu_s'(\mu_s-\mu_s')+\frac{12}{35}(\mu_s-\mu_s')^2-(\tilde{\mu}-\mu_0)^2\right]\right\} \tag{4.31}$$

for shear waves.

The task that remains is to evaluate the structure factors Λ, Λ', which depend upon the function $p(r)$ that appears in (4.2). First, for the function

$$p_1(r) = e^{-r/a}, \tag{4.32}$$

which was introduced by Pekeris[18],

$$\Lambda_1 = 8\pi a^3, \quad \Lambda_1' = 2\pi a^2. \tag{4.33}$$

Table 1. The structure factors Λ, Λ' for the four models, normalized so that Λ, the expected volume of the cell containing the origin, is $4\pi b^3/3$

Model	1	2	3	4
Λ	$4\pi b^3/3$	$4\pi b^3/3$	$4\pi b^3/3$	$4\pi b^3/3$
Λ'	$1.903b^2$	$4.606b^2$	$2.069b^2$	$2.322b^2$

Table 2. Moduli and densities of copper, alpha-iron and nickel

Material	κ_c(GPa)	μ_c(GPa)	μ_c'(GPa)	ρ(g cm^{-3})
Cu	136.7	23.5	75.4	8.95
α-Fe	173.0	48.0	116.0	7.92
Ni	180.4	49.6	124.7	9.04

Table 3. Estimates of wave speeds, with comparison materials chosen as Hashin–Shtrikman lower bounds (H-S lower), self-consistently (S–C) or Hashin–Shtrikman upper bounds (H-S upper)

	Longitudinal wave speed $\tilde{\alpha}$ (mm/μs)			Shear wave speed $\tilde{\beta}$ (mm/μs)		
Material	H-S lower	S-C	H-S upper	H-S lower	S-C	H-S upper
Cu	4.703	4.738	4.758	2.266	2.320	2.350
α-Fe	5.949	5.972	5.986	3.187	3.219	3.239
Ni	5.699	5.724	5.740	3.065	3.100	3.122

Table 4. Estimates of the perturbations Q_1, Q_2, using the Pekeris model for $p(r)$

	$Q_1/(k_1b)^3$			$Q_1'/(k_1b)^2$		
Material	Cu	α-Fe	Ni	Cu	α-Fe	Ni
H-S lower	0.316	0.132	0.148	0.101	0.051	0.057
S-C	0.111	0.061	0.066	0.052	0.031	0.034
H-S upper	0.054	0.035	0.037	0.032	0.022	0.024

Table 5. Estimates of the perturbations Q_2, Q_2', using the Pekeris model for $p(r)$.

	$Q_2/(k_2b)^3$			$Q_2'/(k_2b)^2$		
Material	Cu	α-Fe	Ni	Cu	α-Fe	Ni
H-S lower	0.114	0.053	0.060	0.076	0.039	0.043
S-C	0.041	0.025	0.027	0.040	0.024	0.026
H-S upper	0.020	0.014	0.015	0.025	0.017	0.018

Next, for the function

$$p_2(r) = e^{-(r/a)^2} \tag{4.34}$$

employed by Chernov[19],

$$\Lambda_2 = \pi^{3/2}a^3, \quad \Lambda_2' = \pi a^2. \tag{4.35}$$

These simple expressions are useful for illustrative purposes but they are not associated with any known cell model. Two further examples are therefore considered, for which the functions

$p(r)$ are obtained from explicit stochastic models. They have both been described by Gilbert[10]. In the first of these, points are distributed throughout three-dimensional space, according to a Poisson process of intensity λ, and the space is then partitioned into the convex Dirichlet regions of the points. The Dirichlet region surrounding a given Poisson point consists of the set of points lying nearer to this than any other Poisson point. Gilbert showed that for this model

$$p_3(r) = 2\pi\lambda \int_0^{\pi} d\theta \int_0^{\infty} dR\, R^2 \sin\theta\, e^{-\lambda V(R,\theta)}, \tag{4.36}$$

where $V(R, \theta)$ is the volume of the union of two spheres, one at the origin, with radius R, and the other distant r from the origin, with radius $(R^2+r^2-2Rr\cos\theta)^{1/2}$, θ being measured from the line of centres. For this model, the Poisson points can be thought of as seeds from which cells grow, uniformly in all directions, until they meet at mutual interfaces. The final model, which was introduced by Johnson and Mehl[21], is of the same type, except that a Poisson process on $R^3 \times [0, \infty]$ is considered, which marks the Poisson point P_i with a birth time t_i. It nucleates a cell, therefore, only if it falls in a region not already covered by a cell at time t_i. The Dirichlet cells of the simpler stochastic model are convex polyhedra but those of the Johnson-Mehl model are only star-shaped. Gilbert[20] gives an expression for $p_4(r)$ for the Johnson-Mehl model, in terms of a multiple integral. It is more complicated than (4.36) and is not repeated.

The structure factors Λ, Λ' have been evaluated by Gilbert[20] for each of the Poisson models. The results for all four models are summarized in Table 1 in which, to facilitate comparison, the factor Λ has been normalized as $4\pi b^3/3$: this fixes the lengths a in the first two models and the intensities of the Poisson processes in the other two.

As specific examples, the long-wavelength wave speeds $\tilde{\alpha}$, $\tilde{\beta}$ and the corrections Q', Q giving dispersion and attenuation have been calculated for polycrystalline copper, alpha-iron and nickel. The relevant material properties (taken form[22]) are shown in Table 2. Table 3 gives three estimates for each of $\tilde{\alpha}$, $\tilde{\beta}$, corresponding to choices of comparison material which give, respectively, the Hashin–Shtrikman lower bound, the self-consistent estimate and the Hashin–Shtrikman upper bound for the overall shear modulus. The perturbations Q, Q' are proportional to Λ, Λ' respectively and so depend upon the model chosen for $p(r)$. Table 4 shows estimates of the perturbations Q_1, Q_1' for longitudinal waves, for each choice of comparison material and for the Pekeris form (4.32) for $p_1(r)$. Table 5 gives corresponding estimates of the perturbations Q_2, Q_2' for shear waves. The results are normalized to b (where $\Lambda = 4\pi b^3/3$); in this form, results for Q are independent of the model, while results for Q', for models other than 1, are obtainable by scaling, using Table 1.

5. CONCLUSIONS

Implications of the general formulae in Paper I have been developed for a range of materials displaying overall isotropy. The predicted attenuation and dispersion are sensitive to the choice of comparison material; limited comparison with experimental results tends to favour the self-consistent choice of L_0, though for extreme cases, such as a matrix with a high density of rigid inclusions, or a highly porous medium, the self-consistent L_0 is known to be unsatisfactory and some other choice would be needed.

The analysis shows that attenuation and dispersion depend upon the structure factors Λ', Λ and it should be possible to determine these factors experimentally. For a matrix-inclusion composite, the factors depend upon the radial distribution function as well as the mean inclusion radius and concentration, so that the situation is a little more complicated than was envisaged in [14, 15].

Acknowledgement—One of us (D.R.S.T.) gratefully acknowledges financial support from the Science Research Council.

REFERENCES

1. D. R. S. Talbot and J. R. Willis, *Int. J. Solids Structures* **18**, 673 (1982).
2. V. K. Kinra, M. S. Petraitis and S. K. Datta, *Int. J. Solids Struct.* **16**, 301 (1980).
3. J. R. Willis, *J. Mech. Phys. Solids* **25**, 185 (1977).

4. L. J. Walpole, *J. Mech. Phys. Solids* **14**, 151 (1966).
5. R. Hill, *J. Mech. Phys. Solids* **13**, 89 (1965).
6. J. R. Willis, *J. Mech. Phys. Solids* **28**, 307 (1980).
7. J. K. Percus and G. J. Yevick, *Phys. Rev.* **110**, 1 (1958).
8. M. S. Wertheim, *Phys. Rev. Lett.* **10**, 321 (1963).
9. M. Lax, *Phys. Rev.* **85**, 621 (1952).
10. Z. Hashin and S. Shtrikman, *Phys. Rev.* **11**, 127 (1963).
11. A. V. Hershey, *J. Appl. Mech.* **21**, 236 (1954).
12. R. Hill, *J. Mech. Phys. Solids* **13**, 213 (1965).
13. B. Budiansky, *J. Mech. Phys. Solids* **13**, 223 (1965).
14. C. M. Sayers, *J. Phys. D (Appl. Phys.)* **13**, 179 (1980).
15. C. M. Sayers, *J. Phys. D (Appl. Phys.)* **14**, 413 (1981).
16. L. J. Walpole, *J. Mech. Phys. Solids* **14**, 289 (1966).
17. Z. Hashin and S. Shtrikman, *J. Mech. Phys. Solids* **10**, 343 (1962).
18. C. L. Pekeris, *Phys. Rev.* **7**, 268 (1947).
19. L. A. Chernov, *Wave Propagation in a Random Medium* (Eng. translation by R. A. Silverman). McGraw-Hill, New York (1960).
20. E. N. Gilbert, *Ann. Math. Stat.* **33**, 958 (1962).
21. W. A. Johnson and R. F. Mehl, *Trans. A.I.M.M.E.* **135**, 416 (1939).
22. *American Institute of Physics Handbook* (Edited by D. E. Gray). McGraw-Hill, New York (1972).